Naturally occurring regulatory dendritic cells regulate murine cutaneous chronic graft-versus-host disease

Kaori Sato,[1] Kawori Eizumi,[1] Tomohiro Fukaya,[1] Shigeharu Fujita,[1,2] Yumiko Sato,[1] Hideaki Takagi,[1] Mai Yamamoto,[1] Naohide Yamashita,[2] Atsushi Hijikata,[3] Hiroshi Kitamura,[3] Osamu Ohara,[3] Sho Yamasaki,[4] Takashi Saito,[4] and Katsuaki Sato[1]

[1]Laboratory for Dendritic Cell Immunobiology, RIKEN Research Center for Allergy and Immunology, Kanagawa; [2]Department of Advanced Medical Science, Institute of Medical Science, University of Tokyo, Tokyo; and [3]Laboratory for Immunogenomics and [4]Laboratory for Cell Signaling, RIKEN Research Center for Allergy and Immunology, Kanagawa, Japan

Chronic graft-versus-host disease (cGVHD) is a limiting factor in allogeneic hematopoietic stem cell transplantation (alloHSCT) for the treatment of leukemia and other malignancies. Relative to the process that initiates and promotes cGVHD, the regulation is poorly understood. In this study, we examined the role of naturally occurring regulatory dendritic cells (DC_{regs}) in murine major histocompatibility complex (MHC)-compatible and multiple minor histocompatibility antigen (miHAg)–incompatible model of cGVHD in alloHSCT. DC_{regs} generated from bone marrow in vitro (BM-DC_{regs}) exclusively expressed CD200 receptor 3 (CD200R3), which exerted a suppressive function in the Ag-specific $CD4^+$ T-cell response. $CD49^+CD200R3^+$ cells showed similarities in phenotype and function to BM-DC_{regs}, which formally distinguishes them from other leukocytes, suggesting that they are the natural counterpart of BM-DC_{regs}. Treatment of the recipient mice after alloHSCT with the recipient-type $CD49^+CD200R3^+$ cells as well as BM-DC_{regs} protected against cGVHD, and the protection was associated with the generation of Ag-specific anergic $CD4^+$ T cells as well as $CD4^+CD25^+Foxp3^+$ regulatory T cells (T_{regs}) from donor-derived alloreactive $CD4^+CD25^-Foxp3^-$ T cells. In addition, the depletion of $CD49^+CD200R3^+$ cells before alloHSCT enhanced the progression of cGVHD. In conclusion, $CD49^+CD200R3^+$ cells act as naturally occurring DC_{regs} to regulate the pathogenesis of cGVHD in alloHSCT mediated through the control of the transplanted alloreactive $CD4^+$ T cells. (Blood. 2009;113: 4780-4789)

Introduction

Allogeneic hematopoietic stem cell transplantation is a curative therapy for a variety of hematologic, neoplastic, and genetic disorders.[1-3] However, the application of alloSCT has been limited by the morbidity and mortality of graft-versus-host disease (GVHD).[1-3] GVHD is caused by donor T cells that recognize and react to major histocompatibility complex (MHC) and/or minor histocompatibility antigen (miHAg) differences between donor and recipient. Based on different clinical manifestations and histopathology, GVHD can be divided into acute and chronic types.[3-5] Acute GVHD (aGVHD) targets the skin, gastrointestinal tract, and liver.[3-5] Chronic GVHD (cGVHD) typically results in cutaneous and hepatic fibrosis.[3-5] Although aGVHD and cGVHD are similar in some respects, it seems probable that the 2 diseases have different requirements for initiation and pathogenesis mechanisms. Previous studies have suggested that residual host Ag-presenting cells (APCs) are required to initiate aGVHD mediated by donor-derived $CD8^+$ T cells, whereas either donor or host APCs initiated donor-derived $CD4^+$ T cell–mediated cGVHD in murine allogeneic bone marrow (BM) transplantation (alloBMT).[4,5] Although progress has been made in understanding the pathophysiology and the potential curative therapy of aGVHD, much less is understood about the effective therapy for cGVHD, primarily because of the obscurity of regulation of the pathogenesis of cGVHD.

Dendritic cells (DCs) are specialized APCs that play a dual role in inducing adaptive immune responses and in maintaining self-tolerance.[6-8] DCs consist of heterogeneous subsets, including conventional DCs and plasmacytoid DCs, distinguishable by surface and intracellular phenotypic markers, immunologic function, and anatomic distribution.[6] Immature DCs (iDCs) serve as sentinels, recognizing the presence of invading pathogens through various pattern-recognition receptors, and become mature DCs (mDCs) with the up-regulated expression of MHC and costimulatory molecules under inflammatory conditions.[6] Consequently, mDCs move via the afferent lymphatics into the T-cell area of secondary lymphoid tissues, where they select rare Ag-specific naive T cells and induce their activation and differentiation into effector cells, thereby initiating primary immune responses.[6]

Previous studies have shown that tolerogenic DCs generated by the treatment of iDCs with certain immunosuppressive molecules in vitro and their potential natural counterpart $CD11c^{low}CD45RB^{high}$ DCs prevented an immune response through the induction of interleukin-10 (IL-10)–producing T regulatory type 1 cells and expansion of naturally occurring thymic-derived $CD4^+CD25^+Foxp3^+$ regulatory T cells (nT_{regs}).[9,10] However, the specialized DC subset that drives the conversion of $CD4^+CD25^-Foxp3^-$ T cells to inducible $CD4^+CD25^+Foxp3^+$ T_{regs} (iT_{regs}) remains unclear.[11]

Submitted October 7, 2008; accepted February 8, 2009. Prepublished online as *Blood* First Edition paper, February 19, 2009; DOI 10.1182/blood-2008-10-183145.

The online version of this article contains a data supplement.

The publication costs of this article were defrayed in part by page charge payment. Therefore, and solely to indicate this fact, this article is hereby marked "advertisement" in accordance with 18 USC section 1734.

We have previously reported that regulatory DCs (DC_{regs}) generated from murine BM cells in vitro (BM-DC_{regs}), with a moderately high level of MHC class II but defective in the expression of costimulatory molecules, had a greater capacity to protect mice from various immunopathogenic diseases, including aGVHD and cGVHD, than the classic tolerogenic DCs, mediated through the generation of Ag-specific anergic $CD4^+$ T cells and $CD4^+CD25^+Foxp3^+$ iT_{regs} from $CD4^+CD25^-Foxp3^-$ T cells.[12,13] In the present study, we explored the natural counterpart of BM-DC_{regs} expressing specific markers and the possible role of naturally occurring DC_{regs} in cutaneous cGVHD in MHC-compatible and multiple miHAg-incompatible alloBMT.

Methods

Mice

BALB/c (H-2^d) and C57BL/6 (H-2^b) mice were purchased from Charles River Breeding Laboratories (Portage, MI). B10.D2 mice (H-2^d) were purchased from Jackson Laboratory (Bar Harbor, ME). Ovalbumin (OVA)-specific T-cell receptor (TCR; KJ1-26 clonotype) transgenic *Rag2*$^{+/+}$ DO11.10 BALB/c and *Rag2*$^{-/-}$ DO11.10 BALB/c mice have been described.[13,14] All mice were used between 6 and 10 weeks of age and maintained in specific pathogen–free conditions and in accordance with guidelines of the Institutional Animal Care Committee of the RIKEN Institute.

Preparation of DC subpopulations and leukocytes

DCs generated from murine BM cells in vitro (BM-DCs) were prepared as described previously.[12,13] Briefly, BM-iDCs were generated by culturing BM cells with murine granulocyte-macrophage colony-stimulating factor (20 ng/mL; Wako Pure Chemicals, Osaka, Japan) for 8 days subsequently stimulated with lipopolysaccharide (LPS, 1 μg/mL; Sigma-Aldrich, St Louis, MO) for 24 hours to prepare BM-mDCs. BM-DC_{regs} precursors (BM-preDC_{regs}) were generated by culturing BM cells with murine granulocyte-macrophage colony-stimulating factor (20 ng/mL), murine IL-10 (20 ng/mL, Wako Pure Chemical Industries), and human transforming growth factor (TGF)-β1 (20 ng/mL, Wako Pure Chemical Industries) for 8 days. After being stimulated with LPS (1 μg/mL) for 24 hours, BM-preDC_{regs} were depleted of $CD40^+CD80^+CD86^+$ cells with biotinylated monoclonal antibodies (mAbs) to CD40 (3/23), CD80 (16-10A1), and CD86 (GL1; all from BD Biosciences, San Jose, CA) plus Streptavidin Particles Plus-DM (BD Biosciences) to prepare BM-DC_{regs}. $CD3^+$ cells, $B220^+$ cells, or $CD11b^+$ cells were purified from splenocytes with mouse T Lymphocyte Enrichment Set-DM, mouse B Lymphocyte Enrichment Set-DM, or mouse CD11b Magnetic Particles-DM, respectively (all from BD Biosciences). Leukocytes collected from spleen, peripheral blood, and mesenteric lymph nodes (MLNs) were also depleted of $Fc\epsilon RI\alpha^+$ basophils[15] with biotinylated anti-FcεRIα mAb (MAR-1, eBioscience, San Diego, CA) plus Streptavidin Particles Plus-DM. $CD49b^+$ $Fc\epsilon RI\alpha^-$ cells were purified from splenocytes by AutoMACS with a mouse NK Cell Isolation Kit (all from Miltenyi Biotec, Bergisch Gladbach, Germany). These cells were subsequently labeled with biotinylated anti-CD200R3 mAb (6C4H2) plus streptavidin-phycoerythrin (PE; BD Biosciences), and then sorted by AutoMACS with anti-PE Microbeads (Miltenyi Biotec) into $CD49b^+CD200R3^+$ cells or $CD49b^+CD200R3^-$ cells. For the preparation of splenic classic NK cells, $CD49b^+CD200R3^-$ cells were further depleted of $CD11c^+$ cells using biotinylated anti-CD11c mAbs (HL3, BD Biosciences) plus Streptavidin Particles Plus-DM. Similarly, BM cells were sorted by FACSVantage (BD Biosciences) with allophycocyanin-labeled anti-CD49b mAb (HMα2, BD Biosciences) and PE-labeled anti-FcεRIα mAb (MAR-1, eBioscience) into $CD49b^+$ $Fc\epsilon RI\alpha^-$ cells and $CD49b^+$ $Fc\epsilon RI\alpha^+$ basophils, respectively. $CD11c^+$ cells were purified from splenocytes by AutoMACS with mouse CD11c (N418) Microbeads (Miltenyi Biotec). In some experiments, cells were pulsed with $OVA_{323\text{-}339}$ peptide (OVAp; 10 μM) for 4 hours, washed, and used for subsequent experiments. KJ1-26^+ T cells were purified from splenocytes obtained from *Rag2*$^{+/+}$ DO11.10 BALB/c and *Rag2*$^{-/-}$ DO11.10 BALB/c mice with mouse CD4 T Lymphocyte Enrichment Set-DM (BD Biosciences). Subsequently, KJ1-26^+ T cells were sorted into $CD25^-$ T cells and $CD25^+$ T cells with high purity (> 98%) by AutoMACS with a mouse $CD4^+CD25^+$ Regulatory T Cell Isolation Kit (Miltenyi Biotec).

Semiquantitative RT-PCR

Total RNA from cells (10^6) was extracted with TRIzol (Invitrogen, Carlsbad, CA), and cDNA was synthesized with oligo$(dT)_{20}$ as a primer using the SuperScript III First-Strand Synthesis System for reverse-transcribed polymerase chain reaction (RT-PCR) kit (Invitrogen). PCR analysis was performed using AccuPower PCR PreMix (BIONEER, Daejeon, Korea) with a pair of specific primers for *Cd200r1* (5′-atg ttt tgc ttt tgg aga-3′ and 5′-cta gat tcc aat ggc cga-3′), *Cd200r2* (5′-atg cat gct ttg ggg agg-3′ and 5′-tca tgt tct ggt aac att-3′), *Cd200r3* (5′-atg cat gct ttg ggg agg-3′ and 5′-cta cgt agg agc caa tgt-3′), *Cd200r4* (5′-atg cat gct ctg ggg agg-3′ and 5′-tca tgt tct ggc aaa att-3′), *Gzmb* (5′-aca aca tca aag aac agg aga aga c-3′ and 5′-gct ttt cat tgt ttt ctt tat cca g-3′), *Mcpt8* (5′-ggc ata cat aag gtt taa tga cag c-3′ and 5′-agt cac cct tac cag tag cct tat t-3′), *Tgfb1* (5′-cca tct atg aga aaa cca aag aca t-3′ and 5′-gag ctg aag caa tag ttg gta tcc-3′), and *Actb* (5′-tcc tgt ggc atc cat gaa act-3′ and 5′-gaa gca ctt gcg gtg cac gat-3′). Conditions for the reactions were 30 seconds of denaturation at 94°C, 30 seconds of annealing at 58°C, and 1 minute of elongation at 72°C for 25 cycles (*Actb*) or 30 cycles (*Cd200r1*, *Cd200r2*, *Cd200r3*, *Cd200r4*, *Gzmb*, *Mcpt8, Tgfb1*).

Quantitative TaqMan RT-PCR

cDNA was synthesized with random hexamers as a primer as described in "Semiquantitative RT-PCR". Expression levels of *Cd200r1*, *Cd200r2*, *Cd200r3*, and *Cd200r4* were measured by real-time PCR (7300 Real Time PCR System, Applied Biosystems, Foster City, CA) using TaqMan universal PCR Master Mix (Applied Biosystems) and TaqMan probes mix for *Cd200r1*, *Cd200r2*, *Cd200r3*, and *Cd200r4* (Applied Biosystems) after normalization for the expression of *Actb* (Applied Biosystems).

Retrovirus-mediated gene transfer

The full-length *Cd200*, *Cd200r1*, *Cd200r2*, *Cd200r3*, and *Cd200r4* were amplified by PCR as described in "Semiquantitative RT-PCR" with a pair of specific primers for *Cd200* (5′-cgc *gga tcc* gcc gcc atg ggc agt ctg gta-3′ and 5′-cgc *gaa ttc* tta ttt cat tct ttg cat-3′), *Cd200r1* (5′-cgc *gga tcc* gcc gcc atgt ttt gct ttt gg-3′ and 5′-cgc *gga tcc* cta gat tcc aat ggc cga-3′), *Cd200r2* (5′-tc *gga tcc* gcc gcc atg cat gct ttg ggg agg act ccg-3′ and 5′-tc *gaa ttc* atg ttc tgg taa cat ttc tct tc-3′), *Cd200r3* (5′-cgc *gga tcc* gcc gcc atg cat gct ttg ggg-3′ and 5′-cgc *gga tcc* cta cgt agg agc caa tgt-3′), and *Cd200r4* (5′-tc *gga tcc* gcc gcc atg cat gct ctg ggg agg att ccg-3′ and 5′-tc *gaa ttc* atg ttc tgg caa aat ttc tct tc-3′), and each of the 5′- and 3′-primers was also tagged (indicated in italics) with BamH1 and EcoR1sites for *Cd200, Cd200r2*, and *Cd200r4* or a BamH1 site for *Cd200r1* and *Cd200r3*, respectively. The PCR product was subcloned into pCR4-TOPO using a TA TOPO Cloning Kit for Sequencing (Invitrogen), and the nucleotide sequence was confirmed with an ABI3100xl automated sequencer (Applied Biosystems) and the fluoresceinated dye terminator cycle sequencing method. After restriction enzyme digestion, the DNA sequence was cloned into the sites of the pMX-internal ribosome entry site-green fluorescent protein (GFP) vector[16] and transfected into a retroviral packaging cell line, Phoenix,[16] with LipofectAMIN Plus Reagent (Invitrogen). The culture supernatant of Phoenix after 24 hours of culture was collected and centrifuged at 8000*g* for 16 hours at 4°C to concentrate the virus. The retroviral vector was transfected into RBL2H3 cells together with DOTAP Liposomal Transfection Reagent (Roche Diagnostics, Mannheim, Germany) by centrifugation at 2000*g* for 1 hour at 32°C, and transfectants were subsequently collected for examining GFP expression using FACSVantage. Similarly, BM-iDCs were spin-infected with supernatants containing retrovirus carrying CD200R3-internal ribosome entry site-GFP mixed with polybrene (1 μg/mL; Sigma-Aldrich) on days 2, 3, and 4 according to a previous report.[17] Subsequently,

cells were assayed for the expression CD200R3 and GFP and sorted into $CD200R3^+GFP^+$ and $CD200R3^-GFP^+$BM-iDCs using FACSVantage.

Flow cytometry

Cells were stained with fluorescein-conjugated mAbs to mouse CD3ϵ (145-2C11), CD11b (M1/70), CD11c (HL3), CD40 (3/23), CD49b (HMα2), CD80 (16-10A1), CD86 (GL1), H-$2K^d$ (SF1-1.1), I-A/I-E (M5/114.15.2), B220 (RA3-6B2), Thy1.2 (30-H2), isotype-matched control mAb (all from BD Biosciences), Foxp3 (FJK-16s; eBioscience), CD25 (7D5), mPDCA-1 (JF05-1C2.4.1; both from Miltenyi Biotec), and mouse DO11.10 TCR (KJ1-26; Invitrogen). In another experiment, cells were stained with biotinylated mAbs to CD200R1 (13H6E3), CD200R2 (B2C2F3), CD200R3 (6C4H2), and CD200R4 (8B3C9), which were generated in our laboratory as described in Figure S1 (available on the *Blood* website; see the Supplemental Materials link at the top of the online article), plus streptavidin-PE. Fluorescence staining was analyzed with a FACSCalibur flow cytometer and CELLQuest Software (both from BD Biosciences).

Priming of $CD4^+$ T cells in vitro

Rag2$^{-/-}$$KJ1\text{-}26^+$ T cells (2×10^6) were cultured with the irradiated (15 Gy from a ^{137}Cs source, Gammacell 40 Exactor; MDS Sciex, Concord, ON) OVAp/APCs (2×10^5) in the presence or absence of human TGF-β1 (0.1 ng/mL), anti-TGF-β mAb (1D11, 5 μg/mL), anti-CD200R3 mAb (6A5A8-F7, 5 μg/mL), or control Ig (5 μg/mL) in 6-well flat plates (BD Biosciences) for 6 days, and used in subsequent experiments.

APC assay

Rag2$^{-/-}$$KJ1\text{-}26^+$ T cells (5×10^4) were cultured in 96-well flat-bottomed plates (BD Biosciences) with the irradiated syngeneic OVAp/APCs (6.25×10^2-5×10^3) in the presence or absence of anti-CD200R3 mAb (6A5A8-F7) or control Ig (each 5 μg/mL) for 3 days. We also used irradiated syngeneic hemolyzed splenocytes (5×10^4) cultured in the presence of OVAp (1 μM). Alternatively, huIgFc, CD200ext-huIgFc, CD200R1ext-huIgFc, CD200R2ext-huIgFc, CD200R3ext-huIgFc, CD200R4ext-huIgFc, or CTLA-4ext-huIgFc (R&D Systems, Minneapolis, MN; 5 μg/mL) was added to the culture. [^{3}H]Thymidine (GE Healthcare, Little Chalfont, United Kingdom) incorporation was measured on day 3 for the last 18 hours.

Cell stimulation

$CD11c^+$DCs, $CD49b^+CD200R3^+$ cells or $CD49b^+CD200R3^-$ cells (5×10^5) were cultured with or without LPS (1 μg/mL) or CpG oligodeoxynucleotide (ODN) 1668 (0.1 μM; Hokkaido System Science, Sapporo, Japan) for 24 hours in 24-well plates (BD Biosciences). The culture supernatants were collected and stored at −80°C until assayed for cytokines or morphology was examined by phase-contrast microscopy.

Enzyme-linked immunosorbent assay

Culture supernatants and serum were assayed using enzyme-linked immunosorbent assay kits for mouse IL-12p70, tumor necrosis factor (TNF)-α, IL-10, interferon (IFN)-α, and IFN-γ (all from BioSource International, Camarillo, CA).

Cytotoxicity assay

$CD11c^+$DCs, $CD49b^+CD200R3^-$ cells, or $CD49b^+CD200R3^+$ cells (6.25×10^3-5×10^4) were cultured in 96-well round bottom plates (BD Biosciences) with $Na_2{}^{51}CrO_4$ (NEN; Life Science Products, Frederick, CO)-labeled YAC-1 cells (5×10^3) for 4 hours. Radioactivity of the supernatants was measured, and the percentage specific lysis was calculated. The value of spontaneous release was less than 10% of the total release.

Models for cGVHD and the evaluation

The induction and the evaluation of cGVHD were performed according to previous reports[4,5] with some modifications.[13] In brief, recipient BALB/c mice (10 per group) received a single dose (800 cGy) of lethal total body irradiation (TBI). Three hours after the TBI, all recipients received T cell–depleted BM cells (10^7/mouse) and $CD4^+CD25^-$ T cells (2×10^6/mouse) obtained from B10.D2 mice through a tail vein. The day of transplantation was designated day 0. Subsequently, the transplanted recipient mice received repetitive intravenous injections of BM-DC_{regs}, $CD11c^+$ DCs, and $CD49b^+CD200R3^+$ cells (5×10^5/mouse) obtained from BALB/c mice on days 2, 9, and 16 after transplantation. Alternatively, huIgFc or CD200R3ext-huIgFc (250 μg/mouse) was intravenously administered on days 2, 4, 6, 8, and 10. For the depletion experiments in vivo, the recipient mice were intravenously injected with anti-CD200R3 mAb (6C4H2) or control Ig (each 500 μg/mouse) on days −7, −5, −3, and −1. Recipients were monitored once every day from the day of transplantation to the indicated days after transplantation to determine the incidence and severity of cutaneous cGVHD as well as mobility, diarrhea, and weight loss. The following scoring system for cutaneous cGVHD was used: 0 indicates healthy appearance; 1, skin lesions with alopecia less than 1 cm^2 in area; 2, skin lesions with alopecia 1 to 2 cm^2 in area; 3, skin lesions with alopecia more than 2 cm^2 in area. Incidence was expressed as the percentage of mice that showed clinical manifestations. In another experiment, recipients were killed on day 30 after allogeneic transplantation to obtain spleen and serum.

Adoptive transfer

Generation of $CD4^+CD25^+Foxp3^+$ T_{regs} from $CD4^+CD25^-Foxp3^-$ T cells in vivo was performed according to previous reports.[13] In brief, *Rag2*$^{-/-}$$KJ1\text{-}26^+$ T cells (10^7/mouse) were intravenously transferred with or without OVAp/$CD11c^+$ DCs, OVAp/$CD49b^+CD200R3^-$ cells, or OVAp/$CD49b^+CD200R3^+$ cells (10^6/mouse) into BALB/c mice. After 8 days, $CD4^+$ T cells were purified from the recipient mice as described in "Preparation of DC subpopulations and leukocytes," and the expression of CD25 and Foxp3 among gated $KJ1\text{-}26^+$ T cells was analyzed by flow cytometry. In another experiment, *Rag2*$^{-/-}$$KJ1\text{-}26^+$ T cells and *Rag2*$^{-/-}$$KJ1\text{-}26^+CD25^+$ T cells were isolated from $CD4^+$ T cells and used for subsequent experiments.

Analysis of T_{reg} function

$CD4^+CD25^-$ T cells obtained from B10.D2 mice (5×10^4) were cultured with the irradiated $CD11c^+$ DCs (5×10^3) obtained from BALB/c mice in the presence or absence of $CD4^+CD25^+$ T cells (6.25×10^3-5×10^4) obtained from B10.D2 mice or the transplanted recipient mice in 96-well round bottom plates. Similarly, *Rag2*$^{-/-}$$KJ1\text{-}26^+$ T cells (2×10^4) were cultured with the irradiated splenocytes (2×10^4) plus anti-CD3ϵ mAb (1 μg/mL) in the presence or absence of *Rag2*$^{+/+}$$KJ1\text{-}26^+CD25^+$ T cells obtained from *Rag2*$^{+/+}$ DO11.10 BALB/c mice or *Rag2*$^{-/-}$$KJ1\text{-}26^+CD25^+$ T cells obtained from the adoptively transferred mice (2.5×10^3-2×10^4) in 96-well round bottom plates. The proliferation was evaluated on day 3 based on [^{3}H]thymidine incorporation.

Statistical analysis

Data are the mean plus or minus SEM. All analyses for statistically significant differences were performed with analysis of variance. *P* values less than .01 were considered significant.

Results

Identification of CD200R3 as a specific functional molecule for BM-DC_{regs}

To identify the molecule specifically expressed on BM-DC_{regs}, we screened the transcripts of the potential immunoregulatory cell surface molecules increased in BM-DC_{regs} compared with BM-

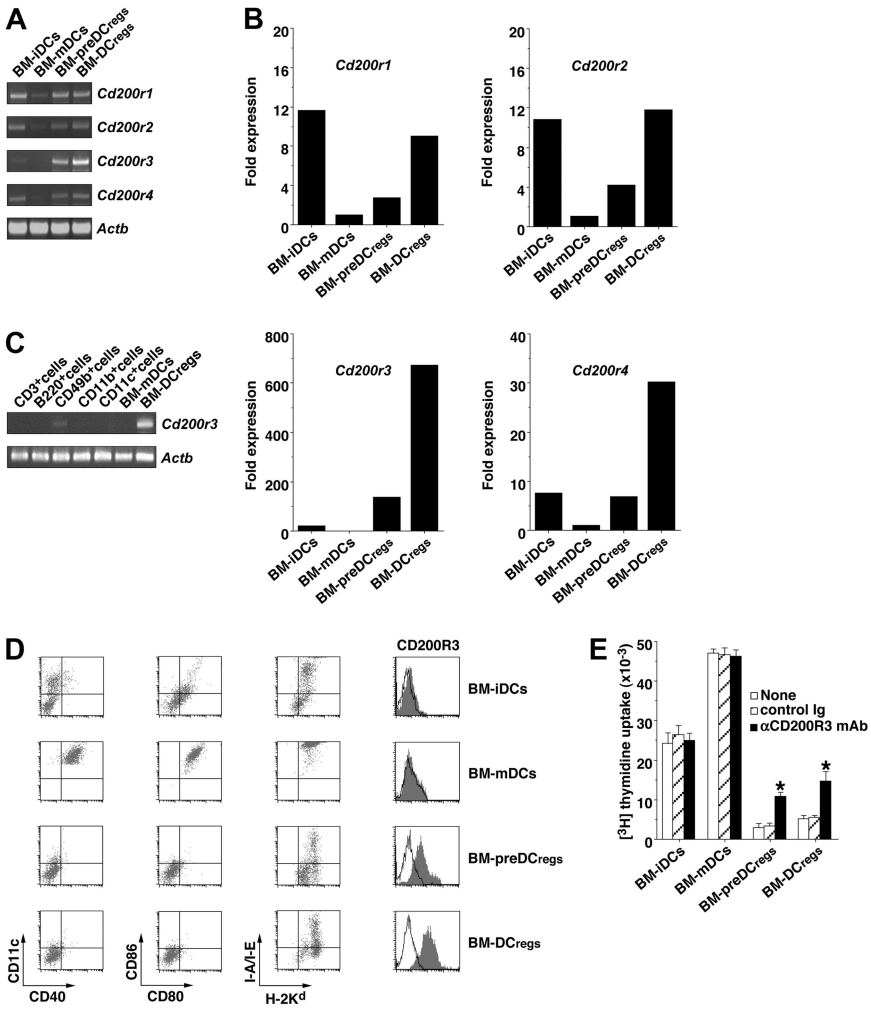

Figure 1. Identification of CD200R3 as a specific molecule for BM-DC$_{regs}$. (A-C) The transcriptional expression of *Cd200r*s in BM-DCs (A,B) and leukocytes (C) was measured by RT-PCR (A,C) and real-time PCR (B). The results of RT-PCR for *Actb* demonstrate the loading of equal amounts of DNA on the gel (A,C). The expression of *Cd200rs* determined by real-time PCR was normalized to that of *Actb*, and the data are as the comparative fold increase compared with BM-mDCs (B). (D) The expression of cell surface molecules on BM-DCs was analyzed by flow cytometry, and data are represented by a dot plot and a histogram. Data are representative of 4 replicate experiments (A-D). (E) *Rag2*$^{-/-}$KJ1-26$^+$ T cells (5×10^4) were cultured with the indicated BM-DCs (5×10^3) in the presence or absence of anti-CD200R3 mAb or control Ig (each 5 μg/mL) for 3 days, and the proliferative response was measured. *$P < .01$ compared with each of the BM-DCs alone. Data are mean ± SEM, and the results are combined from 4 replicate experiments.

mDCs, and identified CD200R family members as candidates (Figure 1A-C). Transcription of *Cd200r3*, but not other *Cd200r*s, was specifically up-regulated in both BM-DC$_{regs}$ and BM-preDC$_{regs}$ compared with both BM-iDCs and BM-mDCs (Figure 1A-C). To analyze the cell surface expression of CD200Rs, we generated mAbs, which specifically recognized each CD200R (Figure S1). BM-preDC$_{regs}$ and BM-DC$_{regs}$ exclusively expressed CD200R3, whereas BM-iDCs and BM-mDCs did not express this molecule (Figure 1D).

We examined the role of CD200R3 in the ability of BM-preDC$_{regs}$ and BM-DC$_{regs}$ to stimulate Ag-specific CD4$^+$ T cells using *Rag2*$^{-/-}$OVA-specific TCR (KJ1-26 clonotype) transgenic mice (DO11.10 mice), which lack CD25$^+$Foxp3$^+$ nT$_{regs}$ (*Rag2*$^{-/-}$KJ1-26$^+$ T cells).[13,14] The ability of OVAp-pulsed BM-preDC$_{regs}$ (OVAp/BM-preDC$_{regs}$) and OVAp/BM-DC$_{regs}$ to stimulate *Rag2*$^{-/-}$KJ1-26$^+$ T cells was much less than that of OVAp/BM-iDCs or OVAp/BM-mDCs (Figure 1E). Anti-CD200R3 mAb partly abrogated the reduced activation of *Rag2*$^{-/-}$KJ1-26$^+$ T cells by OVAp/BM-preDC$_{regs}$ and OVAp/BM-DC$_{regs}$ (Figure 1E).

To address the immunoregulatory function of CD200R3, we fused the extracellular domain of CD200R3 with human IgFc (CD200R3ext-huIgFc). Although CD200ext-huIgFc bound to CD200R1-GFP-RBL2H3 cells and CD200R2-GFP-RBL2H3 cells to a lesser degree, it did not bind to CD200R3-GFP-RBL2H3 cells or CD200R4-GFP-RBL2H3 cells (Figure S2A top panel), and similar results were observed when the binding of each fusion protein to CD200-GFP-RBL2H3 cells was tested (Figure S2A bottom panel). On the other hand, CD200R3ext-huIgFc as well as CD200ext-huIgFc and CTLA-4ext-huIgFc, but not other CD200Rsext-huIgFc, suppressed the activation of *Rag2*$^{-/-}$KJ1-26$^+$ T cells by OVAp/BM-mDCs (Figure S2B).

We also examined the effect of the ectopic expression of CD200R3 on the ability of BM-iDCs to stimulate *Rag2*$^{-/-}$KJ1-26$^+$ T cells. OVAp/CD200R3$^+$GFP$^+$ BM-iDCs generated by retroviral transfection showed the reduced activation of *Rag2*$^{-/-}$KJ1-26$^+$ T cells compared with OVAp/CD200R3$^-$GFP$^-$BM-iDCs and OVAp/CD200R3$^-$GFP$^+$BM-iDCs despite the similar levels of MHC and costimulatory molecules (Figure 2). These results indicate that CD200R3 acts as a suppressive molecule in the Ag-specific response of CD4$^+$ T cells.

Identification of naturally occurring DC$_{regs}$

To clarify the naturally occurring DC$_{regs}$ expressing CD200R3 in vivo, we performed a cytofluorometric analysis of splenocytes. Approximately 0.2% of splenocytes expressed CD200R3 (Figure 3A). In accordance with the transcriptional expression (Figure 1C), CD49b$^+$ cells expressed CD200R3 (Figure 3A), whereas other leukocytes did not express this molecule (data not shown).

Recent studies have shown that CD200R3 was also expressed on FcεRIα$^+$ basophils.[15,18] CD49b$^+$CD200R3$^+$ cells purified from splenocytes consisted of FcεRIα$^-$ cells and FcεRIα$^+$ basophils (Figure 3B); and CD49b$^+$CD200R3$^+$

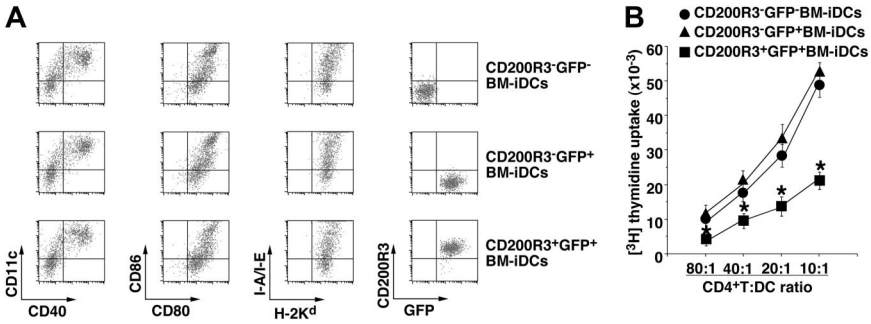

Figure 2. Suppressive function of CD200R3 expressed on DCs in the Ag-specific CD4$^+$ T-cell response. (A) The expression of cell surface molecules on retroviral transfected BM-iDCs was analyzed by flow cytometry, and data are represented by a dot plot. Data are representative of 4 replicate experiments. (B) *Rag2*$^{-/-}$KJ1-26$^+$ T cells (5×10^4) were cultured with OVAp/CD200R3$^-$GFP$^-$BM-iDCs, OVAp/CD200R3$^-$GFP$^+$BM-iDCs, or OVAp/CD200R3$^+$GFP$^+$ BM-iDCs (6.25×10^2-5×10^3) for 3 days, and the proliferative response was measured. * $P < .01$ compared with OVAp/CD200R3$^-$GFP$^-$BM-iDCs. Data are mean ± SEM, and the results are combined from 4 replicate experiments.

FcεRIα$^-$ cells, but not CD49b$^+$CD200R3$^+$ FcεRIα$^+$ basophils, expressed CD11c and I-A/I-E (Figure 3C). In addition, CD49b$^+$CD200R3$^+$ FcεRIα$^-$ cells (referred to as CD49b$^+$CD200R3$^+$ cells) were found in peripheral blood as well as spleen, whereas this cell subset rarely existed in MLNs (Figure 3D) because of a low frequency of CD49b$^+$ cells in LNs under steady-state conditions.[19] CD49b$^+$CD200R3$^+$ cells and BM-DC$_{regs}$ showed similar levels of CD11c, H-2K^d, I-A/I-E, and Thy1.2 with a lack of CD3, CD40, CD80, CD86, B220, and mPDCA-1 known as a marker of plasmacytoid DCs, different from CD11c$^+$ DCs

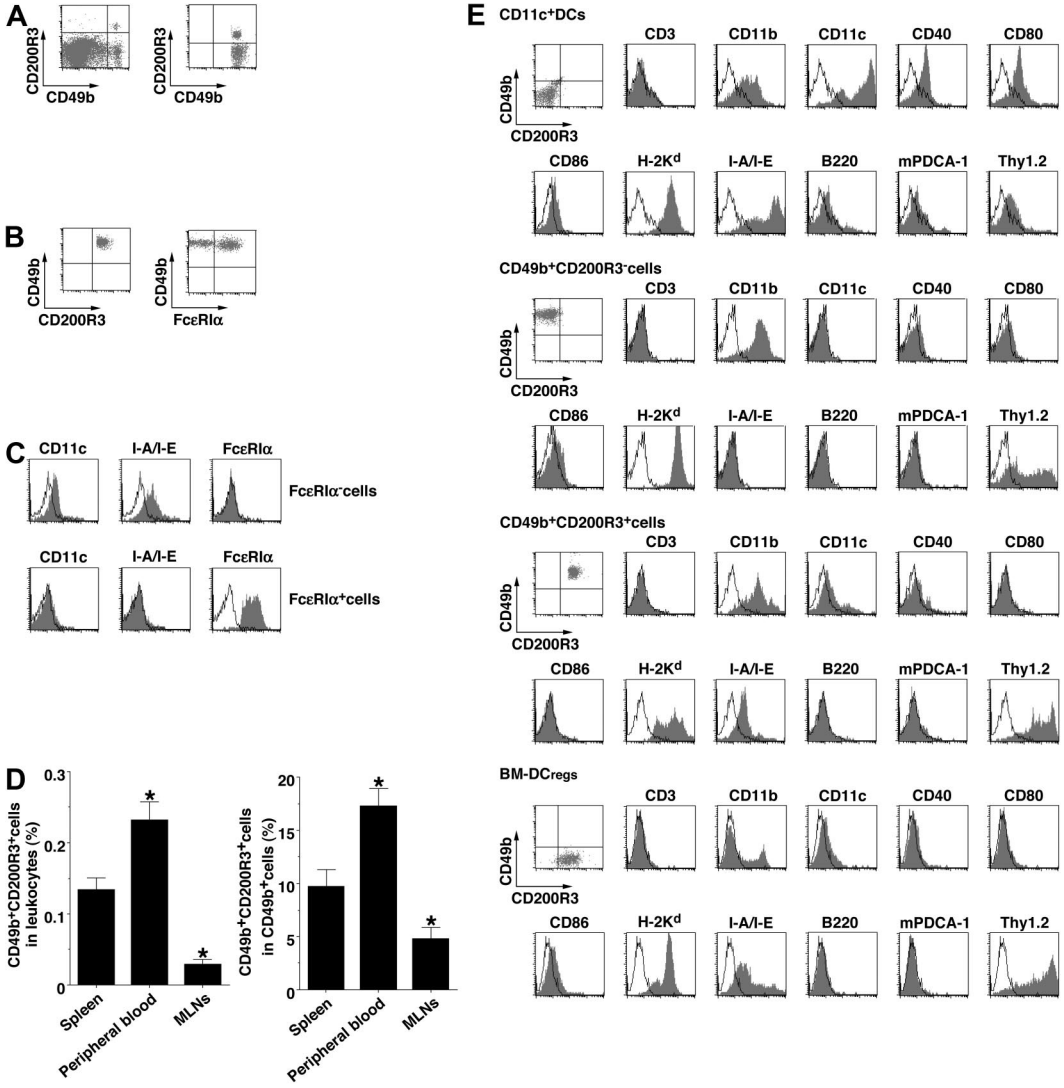

Figure 3. Phenotypic identification of naturally occurring CD49b$^+$CD200R3$^+$ DC$_{regs}$. (A) The expression of CD49b and CD200R3 on splenocyes (left panel) and among gated CD49b$^+$ cells (right panel) was analyzed by flow cytometry, and data are represented by a dot plot. (B) The expression of FcεRIα on CD49b$^+$CD200R3$^+$ cells purified from splenocyes was analyzed by flow cytometry, and data are represented by a dot plot. (C) The expression of CD11c, I-A/I-E, and FcεRIα among gated FcεRIα$^-$ cells and FcεRIα$^+$ cells in CD49b$^+$CD200R3$^+$ cells purified from splenocyes was analyzed by flow cytometry, and data are represented by a histogram. Data are representative of 4 replicate experiments (A-C). (D) CD49b and CD200R3 on leukocytes (left panel) and CD49b$^+$ cells (right panel) from spleen, peripheral blood, and MLNs depleted of FcεRIα$^+$ cells were analyzed by flow cytometry, and data are percentage positive cells. *$P < .01$ compared with splenocytes. Data are mean ± SEM, and the results are combined from 4 replicate experiments. (E) The expression of cell surface molecules on CD11c$^+$ DCs, CD49b$^+$CD200R3$^-$ cells, CD49b$^+$CD200R3$^+$ cells, and BM-DC$_{regs}$ was analyzed by flow cytometry, and data are represented by a dot plot and a histogram. Data are representative of 4 replicate experiments.

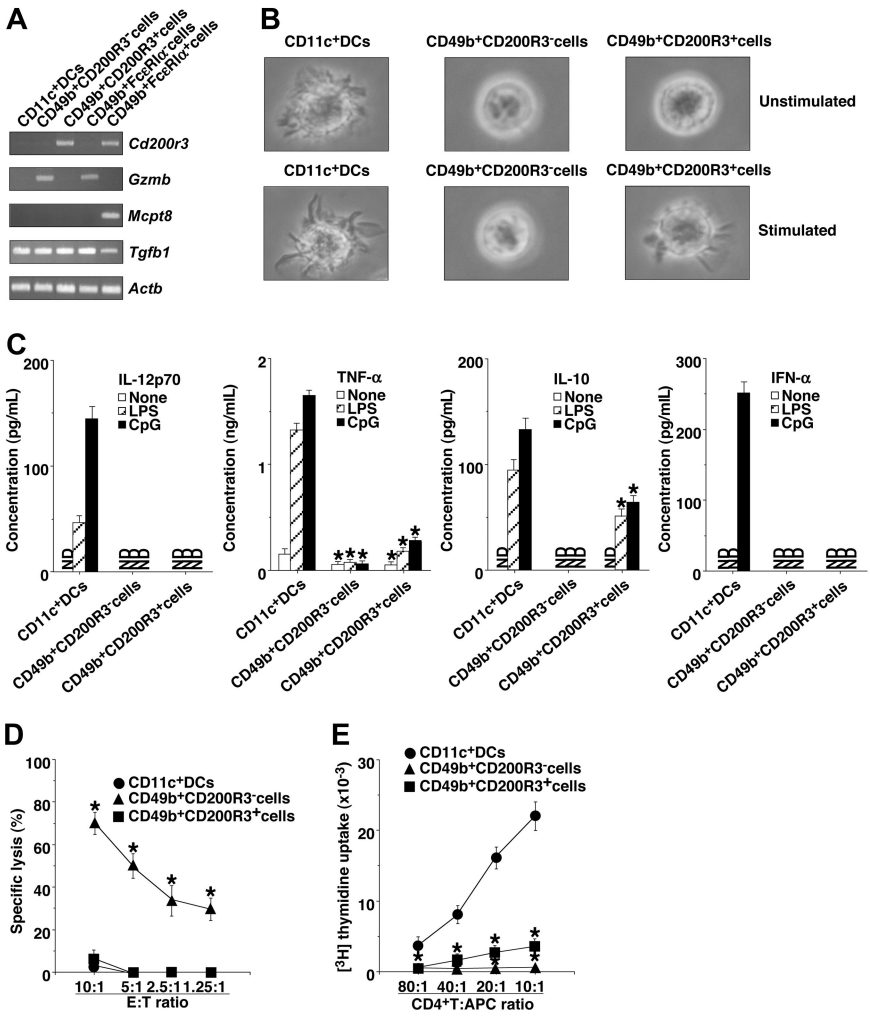

Figure 4. Functional characterization of naturally occurring CD49b$^+$CD200R3$^+$ DC$_{regs}$. (A) The transcriptional expression of the selected genes in CD11c$^+$ DCs, CD49b$^+$CD200R3$^-$ cells, CD49b$^+$CD200R3$^+$ cells, CD49b$^+$FcεRIα$^-$ cells, and CD49b$^+$FcεRIα$^+$ cells was measured by RT-PCR. The results of RT-PCR for *Actb* demonstrate the loading of equal amounts of DNA on the gel. (B) Morphology of CD11c$^+$ DCs, CD49b$^+$CD200R3$^-$ cells, and CD49b$^+$CD200R3$^+$ cells was examined by phase-contrast microscopy (400×) after stimulation with or without CpG ODN (0.1 μM) for 24 hours. Images of micrographs were acquired using a 10 × 20 eyepiece (40 × 0.55 NA objective lenses with phosphate-buffered saline) on an Olympus model CKX41 microscope (Olympus, Yokohama, Japan). An Olympus model DP12-2 camera was used along with JPEG Preview 3.0.9 software (Apple, Cupertino, CA) and Adobe Photoshop Elements 2.0 (Adobe Systems, San Jose, CA) to capture and process the still images. Data are representative of 4 replicate experiments (A,B). (C) CD11c$^+$ DCs, CD49b$^+$CD200R3$^-$ cells, or CD49b$^+$CD200R3$^+$ cells (5×10^5) were stimulated or not stimulated with LPS (1 μg/mL) or CpG ODN (0.1 μM) for 24 hours, and the culture supernatants were analyzed for cytokine production. *$P < .01$ compared with CD11c$^+$ DCs. (D) The cytotoxicity of CD11c$^+$ DCs, CD49b$^+$CD200R3$^-$ cells, or CD49b$^+$CD200R3$^+$ cells (6.25×10^3-5×10^4) against YAC-1 cells (5×10^3) was analyzed by a 4-hour ^{51}Cr release assay. *$P < .01$ compared with CD11c$^+$ DCs. (E) *Rag2*$^{-/-}$KJ1-26$^+$ T cells (5×10^4) were cultured with OVAp/CD11c$^+$ DCs, OVAp/CD49b$^+$CD200R3$^-$ cells, or OVAp/CD49b$^+$CD200R3$^+$ cells (6.25×10^2-5×10^3) for 3 days, and the proliferative response was measured. *$P < .01$ compared with OVAp/CD11c$^+$ DCs. Data are mean ± SEM, and the results are combined from 4 replicate experiments (C-E).

and classic NK cells (CD3$^-$B220$^-$CD11c$^-$CD49b$^+$CD200R3$^-$ cells; Figure 3E).

Functional characterization of naturally occurring DC$_{regs}$

We examined the characteristic features of CD49b$^+$CD200R3$^+$ cells. CD49b$^+$CD200R3$^+$ cells exhibited a distinct transcriptional expression of *Cd200r3*, *Gzmb*, *Mcpt8*,[20] and *Tgfb1* from CD11c$^+$ DCs, NK cells, and basophils (Figure 4A). Stimulation with CpG ODN 1668 induced the morphologic change of CD49b$^+$CD200R3$^+$ cells, but not NK cells, with dendrites resembling those of CD11c$^+$ DCs (Figure 4B). Relative to CD11c$^+$ DCs, which secreted IL-12p70, TNF-α, IL-10, and IFN-α on activation with LPS or CpG ODN, CD49b$^+$CD200R3$^+$ cells produced mostly IL-10 and some proinflammatory cytokines similar to BM-DC$_{regs}$ in our previous reports,[21,22] and NK cells did not produce much of either. NK cells efficiently killed YAC-1 cells, whereas neither CD49b$^+$CD200R3$^+$ cells nor CD11c$^+$ DCs were able to kill YAC-1 cells (Figure 4D). On the other hand, OVAp/CD49b$^+$CD200R3$^+$ cells induced less Ag-specific activation of *Rag2*$^{-/-}$KJ1-26$^+$ T cells than OVAp/CD11c$^+$ DCs, whereas OVAp/NK cells failed to activate them (Figure 4E) because of a lack of MHC class II (Figure 3E).

Naturally occurring DC$_{regs}$ protect the recipients of allogeneic BMT from cutaneous cGVHD

Recipient BALB/c mice transplanted with MHC-compatible (H-2^d) and miHAg-incompatible BM cells and CD4$^+$CD25$^-$ T cells obtained from B10.D2 mice showed clinical features of cutaneous cGVHD, including skin lesions with alopecia, lower mobility, diarrhea, and weight loss,[13] until 33 days after alloBMT (Figure 5). Treatment with the recipient-type CD11c$^+$ DCs slightly enhanced the incidence and severity of cutaneous cGVHD compared with the untreated recipient mice (Figure 5A,B). In contrast, treatment with the recipient-type CD49b$^+$CD200R3$^+$ cells as well as BM-DC$_{regs}$[13] significantly suppressed the incidence and severity of cutaneous cGVHD, whereas CD200R3ext-huIgFc showed a partial protective effect, compared with the untreated recipient mice ($P < .01$; Figure 5A,B).

We also examined serum levels of TNF-α, IL-12p70, and IFN-γ in the transplanted recipient mice (Figure 6A). Treatment with the recipient-type CD11c$^+$ DCs enhanced serum production of these proinflammatory cytokines compared with levels in the untreated recipient mice. In contrast, treatment with the recipient-type CD49b$^+$CD200R3$^+$ cells and BM-DC$_{regs}$[13] as well as CD200R3ext-huIgFc significantly inhibited serum levels of these proinflammatory cytokines.

To clarify the mechanism responsible for the regulation of cutaneous cGVHD, we analyzed donor-derived CD4$^+$ T cells obtained from the transplanted recipient mice. Approximately 98% of spleen mononuclear cells had disappeared by day 5 after TBI, whereas spleen CD4$^+$ T cells were apparently detected in the recipient mice 5 days after alloBMT, indicating that a large proportion of CD4$^+$ T cells observed in the irradiated recipients of

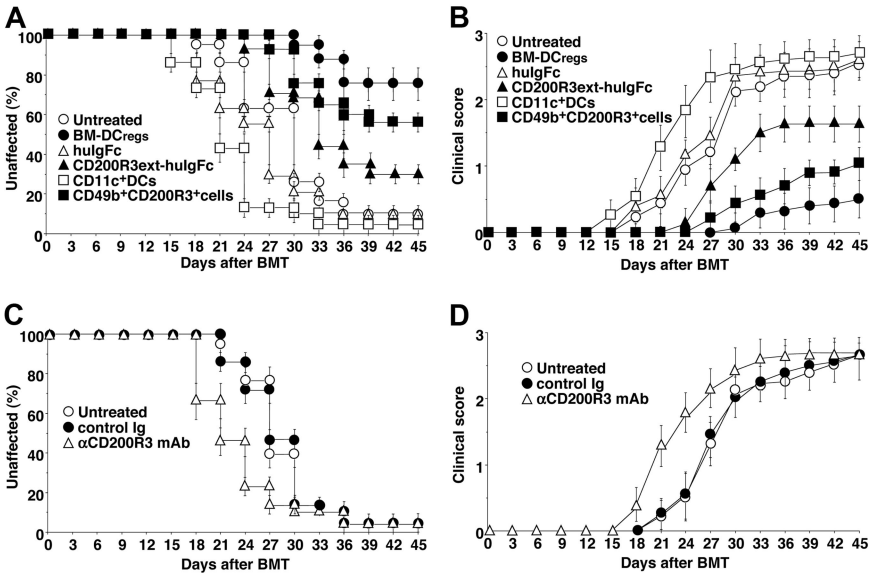

Figure 5. Naturally occurring CD49b$^+$CD200R3$^+$ DC$_{regs}$ protect mice from the incidence and severity of cutaneous cGVHD. (A,B) The irradiated recipient BALB/c mice (10 per group) were transplanted with T cell–depleted BM cells and CD4$^+$CD25$^-$ T cells obtained from B10.D2 mice and then treated with or without the recipient-type BM-DC$_{regs,}$ CD11c$^+$ DCs, CD49b$^+$CD200R3$^+$ cells, huIgFc, or CD200R3ext-huIgFc after the transplantation. The incidence (A) and severity (B) of cutaneous cGVHD were monitored for 45 days after the transplantation. *$P < .01$ compared with the untreated recipient mice. (C,D) The irradiated recipient BALB/c mice that had received anti-CD200R3 mAb or control Ig (10 per group) were transplanted with T cell–depleted BM cells and CD4$^+$CD25$^-$ T cells obtained from B10.D2 mice. The incidence (C) and severity (D) of cutaneous cGVHD were monitored for 45 days after the transplantation. *$P < .01$ compared with the untreated recipient mice. Data are mean ± SEM, and the results are combined from 3 replicate experiments (A-D).

allogeneic transplantation were mainly of donor origin.[13] Donor-derived CD4$^+$ T cells obtained from the recipient mice treated with recipient-type CD11c$^+$ DCs showed a more vigorous response to the recall stimulation with the recipient-type CD11c$^+$ DCs than those obtained from the untreated recipient mice (Figure 6B). In contrast, donor-derived CD4$^+$ T cells obtained from the recipient mice treated with the recipient-type CD49b$^+$CD200R3$^+$ cells and BM-DC$_{regs}$[13] as well as CD200R3ext-huIgFc were hyporesponsive to the recall stimulation with the recipient-type CD11c$^+$ DCs, whereas similar allogeneic response was observed when they were stimulated with CD11c$^+$ DCs obtained from MHC-mismatched strains

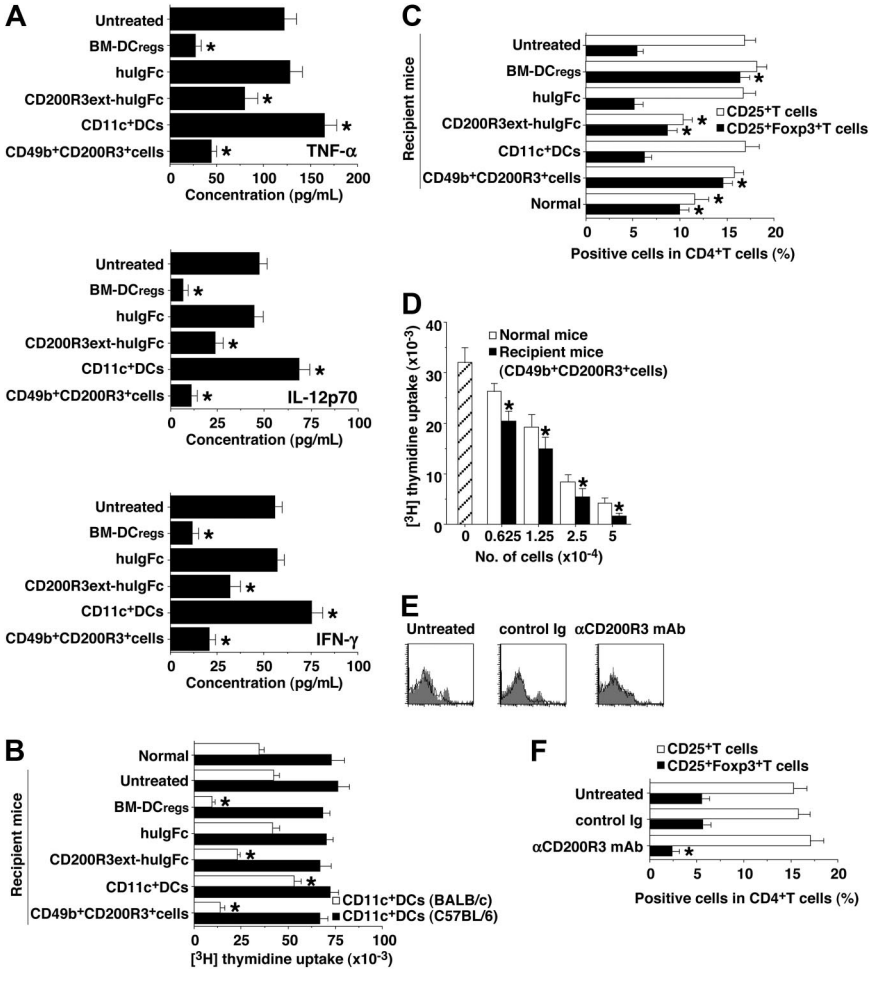

Figure 6. Naturally occurring CD49b$^+$CD200R3$^+$ DC$_{regs}$ induce donor-derived alloreactive CD4$^+$CD25$^+$Foxp3$^+$ T$_{regs}$ in the transplanted recipient mice. (A-D) The transplanted recipient BALB/c mice were prepared as described in Figure 5A and B. Subsequently, serum and donor-derived CD4$^+$ T cells were collected from each transplanted recipient mouse on day 30 after transplantation. (A) Serum production of TNF-α, IL-12p70, and IFN-γ was measured by enzyme-linked immunosorbent assay. *$P < .01$ compared with the untreated group. (B) Donor-derived CD4$^+$ T cells (2×10^5) were cultured with the irradiated CD11c$^+$ DCs (2×10^4) obtained from BALB/c or C57BL/6 mice for 3 days, and the proliferative response was measured. *$P < .01$ compared with normal mice. (C) The expression of CD25 and Foxp3 on CD4$^+$ T cells was analyzed by flow cytometry, and data are percentage positive cells. *$P < .01$ compared with the untreated recipient mice. (D) CD4$^+$CD25$^-$ T cells obtained from B10.D2 mice (5×10^4) were cultured with CD11c$^+$ DCs from BALB/c mice (5×10^3) in the presence of a graded dose (6.25×10^3-5×10^4) of CD4$^+$CD25$^+$ T cells obtained from normal B10.D2 mice (normal mice) or the recipient mice treated with CD49b$^+$CD200R3$^+$ cells for 3 days, and the proliferative response was measured. *$P < .01$ compared with normal mice. Data are expressed as mean plus or minus SEM, and the results are combined from 3 replicate experiments (A-D). (E,F) The transplanted recipient BALB/c mice were prepared as described in Figure 5C and D. (E) The expression of CD200R3 among gated CD49b$^+$ cells was analyzed on day 0 by flow cytometry, and data are represented by a histogram. Data are representative of 3 replicate experiments. (F) Donor-derived CD4$^+$ T cells were collected from each transplanted recipient mouse on day 30 after transplantation. The expression of CD25 and Foxp3 on CD4$^+$ T cells was analyzed by flow cytometry, and data are percentage positive cells. *$P < .01$ compared with the untreated recipient mice. Data are mean ± SEM, and the results are combined from 3 replicate experiments.

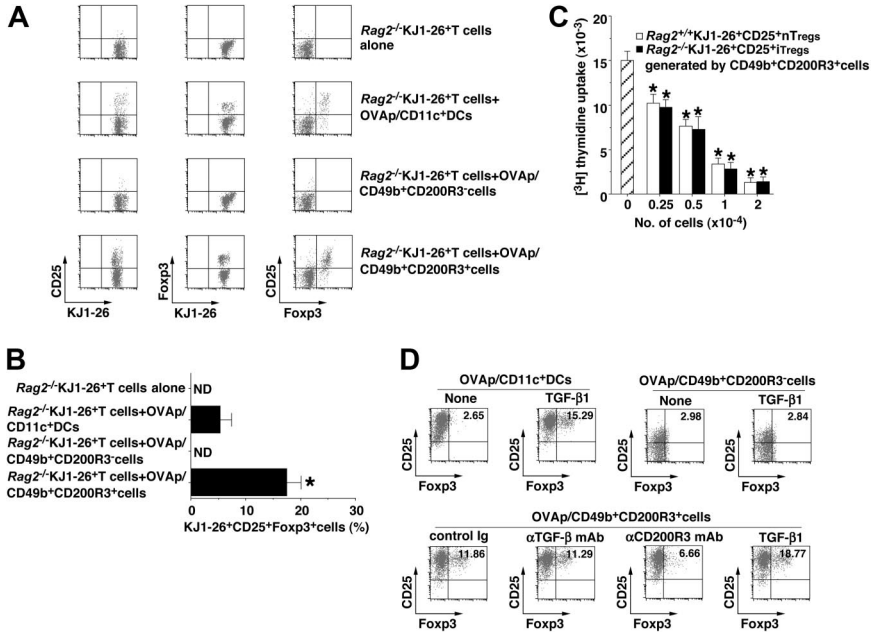

Figure 7. Generation of CD4$^+$CD25$^+$Foxp3$^+$ iT$_{regs}$ from CD4$^+$CD25$^-$Foxp3$^-$ T cells by naturally occurring CD49b$^+$CD200R3$^+$ DC$_{regs}$. (A-C) *Rag2*$^{-/-}$KJ1-26$^+$ T cells (10^7/mouse) were transferred with or without OVAp/CD11c$^+$ DCs, OVAp/CD49b$^+$CD200R3$^-$ cells, or OVAp/CD49b$^+$CD200R3$^+$ cells (10^6/mouse) into mice. On day 8 after the adoptive transfer, *Rag2*$^{-/-}$KJ1-26$^+$ T cells were isolated from the recipient mice. (A,B) The expression of CD25 and Foxp3 among gated KJ1-26$^+$ T cells was analyzed by flow cytometry, and data are represented by a dot plot (A) and are percentage positive cells (B). *$P < .01$ compared with *Rag2*$^{-/-}$KJ1-26$^+$ T cells and OVAp/CD11c$^+$ DCs. Data are representative of 4 replicate experiments (A). Data are mean ± SEM, and the results are combined from 4 replicate experiments (B). (C) *Rag2*$^{-/-}$KJ1-26$^+$ T cells (2×10^4) were cultured with splenocytes (2×10^4) plus anti-CD3ε mAb (1 μg/mL) in the presence of a graded dose (2.5×10^3-2×10^4) of *Rag2*$^{+/+}$KJ1-26$^+$CD25$^+$ T cells or *Rag2*$^{-/-}$KJ1-26$^+$CD25$^+$ T cells obtained from the adoptively transferred mice for 3 days, and the proliferative response was measured. *$P < .01$ compared with *Rag2*$^{-/-}$KJ1-26$^+$ T cells. Data are mean ± SEM, and the results are combined from 4 replicate experiments. (D) *Rag2*$^{-/-}$KJ1-26$^+$ T cells (2×10^6) were cultured with OVAp/CD11c$^+$ DCs, OVAp/CD49b$^+$CD200R3$^-$ cells, or OVAp/CD49b$^+$CD200R3$^+$ cells (2×10^5) in the presence or absence of TGF-β1 (0.1 ng/mL), anti–TGF-β mAb, anti-CD200R3 mAb, or control Ig (each 5 μg/mL) for 6 days, and the expression of CD25 and Foxp3 among gated KJ1-26$^+$ T cells was analyzed by flow cytometry. Data are represented by a dot plot, and numbers represent the percentage of CD25$^+$Foxp3$^+$ cells among gated KJ1-26$^+$ T cells. Data are representative of 4 replicate experiments.

(H-2^b; Figure 6B), indicating that this suppression occurred in an allogeneic Ag-specific manner.

We also examined the generation of donor-derived CD4$^+$CD25$^+$Foxp3$^+$ T cells in the transplanted recipient mice. Flow cytometric analysis showed that CD4$^+$CD25$^+$ T cells were increased, whereas CD4$^+$CD25$^+$Foxp3$^+$ T cells were decreased in number in both the untreated and the recipient mice treated with the recipient-type CD11c$^+$ DCs compared with normal mice (Figure 6C). In contrast, the recipient mice treated with the recipient-type CD49b$^+$CD200R3$^+$ cells and BM-DC$_{regs}$[13] had a larger proportion of CD4$^+$CD25$^+$Foxp3$^+$ T cells than the untreated recipient mice (Figure 6C), and CD4$^+$CD25$^+$ T cells obtained from the recipient mice treated with the recipient-type CD49b$^+$CD200R3$^+$ cells showed greater suppression of the allogeneic activation of CD4$^+$CD25$^-$ T cells than donor-type CD4$^+$CD25$^+$ nT$_{regs}$ (Figure 6D). On the other hand, depletion of CD200R3$^+$ cells by anti-CD200R3 mAb (Figure 6E) before alloBMT not only reduced the generation of CD4$^+$CD25$^+$Foxp3$^+$ T cells (Figure 6F) but also enhanced the progression of cutaneous cGVHD ($P < .01$, Figure 5C,D).

Conversion of CD4$^+$CD25$^-$Foxp3$^-$ T cells to CD4$^+$CD25$^+$Foxp3$^+$ iT$_{regs}$ by naturally occurring DC$_{regs}$

To clarify the role of the recipient-type CD49b$^+$CD200R3$^+$ cells in the production of alloreactive donor-derived CD4$^+$CD25$^+$Foxp3$^+$ T$_{reg}$ in the transplanted recipient mice, we examined the ability of CD49b$^+$CD200R3$^+$ cells to generate CD4$^+$CD25$^+$Foxp3$^+$ iT$_{regs}$ from CD4$^+$CD25$^-$Foxp3$^-$ T cells using the adoptive transfer experiment. The adoptive transfer of *Rag2*$^{-/-}$KJ1-26$^+$CD25$^-$Foxp3$^-$ T cells alone or *Rag2*$^{-/-}$KJ1-26$^+$CD25$^-$Foxp3$^-$ T cells plus OVAp/NK cells did not induce *Rag2*$^{-/-}$KJ1-26$^+$CD25$^+$Foxp3$^+$ T cells (Figure 7A,B). On the other hand, OVAp/CD49b$^+$CD200R3$^+$ cells generated *Rag2*$^{-/-}$KJ1-26$^+$CD25$^+$Foxp3$^+$ T cells from *Rag2*$^{-/-}$KJ1-26$^+$CD25$^-$Foxp3$^-$ T cells more than OVAp/CD11c$^+$ DCs (Figure 7A,B). In addition, *Rag2*$^{-/-}$KJ1-26$^+$CD25$^+$ T cells generated by OVAp/CD49b$^+$CD200R3$^+$ cells exerted the equivalent regulatory function to KJ1-26$^+$CD25$^+$ nT$_{regs}$ isolated from *Rag2*$^{+/+}$ DO11.10 mice (Figure 7C), indicating that they could be iT$_{regs}$. We also showed that OVAp/CD49b$^+$CD200R3$^+$ cells generated *Rag2*$^{-/-}$KJ1-26$^+$CD25$^+$Foxp3$^+$ T cells from *Rag2*$^{-/-}$KJ1-26$^+$CD25$^-$Foxp3$^-$ T cells in vitro, and this conversion was partly blocked by anti-CD200R3 mAb, but not anti–TGF-β mAb (Figure 7D). Furthermore, exogenous TGF-β1 enhanced the generation of *Rag2*$^{-/-}$KJ1-26$^+$CD25$^+$Foxp3$^+$ T cells by OVAp/CD49b$^+$CD200R3$^+$ cells, which was similar to OVAp/CD11c$^+$ DCs plus TGF-β1 (Figure 7D).

Discussion

cGVHD is an increasingly frequent complication of alloBMT.[3-5] Despite a better understanding of the suppression of aGVHD, how cGVHD is regulated remains unclear. Here we report the crucial role of naturally occurring CD49b$^+$CD200R3$^+$ DC$_{regs}$ in the regulation of cutaneous cGVHD in an MHC-compatible and miHAg-incompatible model of murine alloBMT possibly mediated through the generation of alloreactive CD4$^+$CD25$^+$Foxp3$^+$ T$_{regs}$ from donor-derived CD4$^+$CD25$^-$Foxp3$^-$ T cells.

We showed that BM-DC$_{regs}$ exhibited an extremely higher transcriptional and cell surface expression of CD200R3 than their conventional counterparts, suggesting that CD200R3 is a specific molecule for BM-DC$_{regs}$. On the other hand, the defective activation of

Ag-specific $CD4^+$ T cells by BM-DC_{regs} was partly abrogated by anti-CD200R3 mAb. In addition, the analysis with CD200R3ext-huIgFc and CD200R3-transduced BM-iDCs revealed that CD200R3 directly regulated the activation of Ag-specific $CD4^+$ T cells. BM-DC_{regs} had relatively high levels of MHC class II and extremely low levels of costimulatory molecules, and this unique expression profile could deliver a sufficient antigenic signal plus a poor costimulation to Ag-specific $CD4^+$ T cells, which could be involved in the induction of clonal T-cell anergy.[12,23] Therefore, CD200R3 and the default Ag-presentation machinery could mediate the T-cell regulatory function of BM-DC_{regs}.

It has been suggested that binding of CD200 to CD200R imparts a unidirectional negative signal to CD200R-expressing leukocytes, whereas there seems to be no direct effect on cells expressing CD200, which does not contain signaling motifs or docking domains in its short cytoplasmic tail.[24] In accordance with recent reports,[15,25] CD200 could not be a ligand for CD200R3 and CD200R4, although CD200R1 and CD200R2 could be a high and low affinity receptor for CD200, respectively. We also observed that CD200R3ext-huIgFc not only specifically bound to $CD4^+$ T cells and the 2B4 T-cell line but also suppressed intracellular signaling events involving ERK, p38, JNK, and IkBα when they were stimulated with mAbs to CD3ϵ and CD28 (our unpublished data). Although the detailed mechanism of how CD200R3 regulates T-cell function remains a key question for future studies, the engagement of the possible ligand expressed on $CD4^+$ T cells by CD200R3 might trigger the impaired intracellular signaling events leading to the induction of the anergic state. Further investigation regarding the identification of the CD200R3 ligand is being conducted in our laboratories.

$CD49b^+CD200R3^+$ cells showed similarities in phenotype and function to BM-DC_{regs}, which formally distinguishes them from other leukocytes, suggesting that they are the natural counterpart of BM-DC_{regs}. In addition, $CD49b^+CD200R3^+$ cells could more efficiently convert $CD4^+CD25^-Foxp3^-$ T cells into $CD4^+CD25^+Foxp3^+$ iT_{regs} than $CD11c^+$ DCs. Unlike $CD11c^+$ DCs, which required TGF-β for the generation of $CD4^+CD25^+Foxp3^+$ iT_{regs},[26,27] $CD49b^+CD200R3^+$ cells as well as BM-DC_{regs}[13] induced the conversion of $CD4^+CD25^-Foxp3^-$ T cells to $CD4^+CD25^+Foxp3^+$ iT_{regs} in a TGF-β-independent manner, whereas anti-CD200R3 mAb partly suppressed this conversion. Therefore, the generation of $CD4^+CD25^+Foxp3^+$ iT_{regs} by $CD49b^+CD200R3^+$ cells could involve MHC class II and CD200R3, and the additional molecule(s) might be required for this conversion. CD200R3 contains the positively charged amino acid lysine in the transmembrane region, which has the potential to associate with the immunoreceptor tyrosine-activation motif-bearing adaptor molecule DAP12, suggesting that the CD200R3/DAP12 complex can transduce activating signals on basophils and mast cells.[15,18] Indeed, we observed the association of CD200R3 with DAP12 in BM-DC_{regs} (data not shown). However, the treatment with anti-CD200R3 mAb did not enhance the expression of CD80 and CD86 on $CD49b^+$ $CD200R3^+$ cells and BM-DC_{regs} (data not shown). These phenomena might rule out the possibility that the ligation of CD200R3 expressed on $CD49b^+CD200R3^+$ cells by anti-CD200R3 mAb could transduce activating signals, resulting in the abrogation of other molecular events involving the generation of $CD4^+CD25^+Foxp3^+$ iT_{regs}.

The crucial role of either donor- or host-derived APCs in the activation of donor-derived $CD4^+$ T cells has been reported in murine model of cGVHD.[4,5] Similar to the recipient-type BM-mDCs,[13] treatment with the recipient-type $CD11c^+$ DCs after alloBMT slightly promoted the progression of cutaneous cGVHD. In addition, these recipient mice exhibited the enhanced secretion of serum proinflammatory cytokines and alloreactive response of donor-derived $CD4^+$ T cells. These phenomena imply that host residual $CD11c^+$ DCs could be activated under inflammatory conditions to expand the pathogenic donor-derived $CD4^+$ T cells, which lead to promotion of the pathogenesis of cutaneous cGVHD.

We showed that the recipient-type $CD49b^+CD200R3^+$ cells and BM-DC_{regs} as well as CD200R3ext-huIgFc suppressed the progression of cutaneous cGVHD, and the protective effect was correlated with the reduced production of serum proinflammatory cytokines and the impaired alloreactive response of donor-derived $CD4^+$ T cells. Furthermore, the protected recipient mice showed the enhanced production of donor-derived $CD4^+CD25^+Foxp3^+$ T_{regs}, which exerted a more potent regulatory function against the allogeneic activation of donor-type $CD4^+CD25^-$ T cells than donor-type $CD4^+CD25^+Foxp3^+$ T_{regs}. On the other hand, the depletion of $CD200R3^+$cells by anti-CD200R3 mAb before alloBMT resulted in the reduction of donor-derived $CD4^+CD25^+$ $Foxp3^+$ T cells as well as the enhanced progression of cutaneous cGVHD. Collectively, host residual $CD49b^+CD200R3^+$ cells could serve as sentinels, damping donor-derived alloreactive $CD4^+$ T cells mediated through the generation of donor-derived alloreactive $CD4^+CD25^+Foxp3^+$ iT_{regs}, resulting in protection against cutaneous cGVHD.

In conclusion, the findings reported here highlight a functional identification of naturally occurring $CD49b^+CD200R3^+$ DC_{regs} acting to regulate cutaneous cGVHD in an MHC-compatible and miHAg-incompatible murine allogeneic BMT. The functional identification of naturally occurring human DC_{regs} and their modulation in vivo as well as the availability of human DC_{regs} generated in vitro[28] may provide an advantageous means of Ag-specific intervention for cGVHD in alloBMT.

Acknowledgments

The authors thank Drs S. Ishido and J. Shinga for valuable advice on making the vector constructs and all members of the Central Facility at the RIKEN Research Center for Allergy and Immunology for technical help in cell sorting.

This work was supported by Grants-in-Aid for Scientific Research from the Ministry of Education, Science and Culture of Japan (c 17790334 and 19590505; Kat. Sato).

Authorship

Contribution: Kao. Sato designed the research project, analyzed data, and wrote the paper; Kat. Sato, K.E., T.F., S.F., Y.S., H.T., and M.Y. performed the experiments; and N.Y., A.H., H.K., O.O., S.Y., and T.S. contributed vital new reagents or analytical tools.

Conflict-of-interest disclosure: The authors declare no competing financial interests.

Correspondence: Katsuaki Sato, Laboratory for Dendritic Cell Immunobiology, Research Center for Allergy and Immunology, RIKEN Yokohama Institute, Suehiro-cho 1-7-22, Tsurumi, Yokohama, Kanagawa 230-0045 Japan; e-mail: katsuaki@rcai.riken.jp.

References

1. Matte CC, Liu J, Cormier J, et al. Donor APCs are required for maximal GVHD but not for GVL. Nat Med. 2004;10:987-992.
2. Shlomchik WD. Graft-versus-host disease. Nat Rev Immunol. 2007;7:340-352.
3. Baird K, Pavletic SZ. Chronic graft versus host disease. Curr Opin Hematol. 2006;13:426-435.
4. Anderson BE, McNiff JM, Matte C, et al. Recipient $CD4^+$ T cells that survive irradiation regulate chronic graft-versus-host disease. Blood. 2004; 104:1565-1573.
5. Anderson BE, McNiff JM, Jain D, et al. Distinct roles for donor- and host-derived antigen-presenting cells and costimulatory molecules in murine chronic graft-versus-host disease: requirements depend on target organ. Blood. 2005;105: 2227-2234.
6. Sato K, Fujita S. Dendritic cells: nature and classification. Allergol Int. 2007;56:183-191.
7. Steinman RM, Nussenzweig MC. Avoiding horror autotoxicus: the importance of dendritic cells in peripheral T cell tolerance. Proc Natl Acad Sci U S A. 2002;99:351-358.
8. Kretschmer K, Apostolou I, Hawiger D, et al. Inducing and expanding regulatory T cell populations by foreign antigen. Nat Immunol. 2005;6: 1219-1227.
9. Morelli AE, Thomson AW. Tolerogenic dendritic cells and the quest for transplant tolerance. Nat Rev Immunol. 2007;7:610-621.
10. Wakkach A, Fournier N, Brun V, et al. Characterization of dendritic cells that induce tolerance and T regulatory 1 cells differentiation in vivo. Immunity. 2003;18:605-617.
11. Wing K, Fehervari Z, Sakaguchi S. Emerging possibilities in the development and function of regulatory T cells. Int Immunol. 2006;18:991-1000.
12. Sato K, Yamashita N, Yamashita N, Baba M, Matsuyama T. Regulatory dendritic cells protect mice from murine acute graft-versus-host disease and leukemia relapse. Immunity. 2003;18:367-379.
13. Fujita S, Sato Y, Sato K, et al. Regulatory dendritic cells protect against cutaneous chronic graft-versus-host disease mediated through $CD4^+CD25^+Foxp3^+$ T cells. Blood. 2007;110: 3793-3803.
14. Hori S, Nomura T, Sakaguchi S. Control of regulatory T cell development by the transcription factor Foxp3. Science. 2003;299:1057-1061.
15. Kojima T, Obata K, Mukai K, et al. Mast cells and basophils are selectively activated in vitro and in vivo through CD200R3 in an IgE-independent manner. J Immunol. 2007;179:7093-7100.
16. Yokosuka T, Takase K, Suzuki M, et al. Predominant role of T cell receptor (TCR)-α chain in forming preimmune TCR repertoire revealed by clonal TCR reconstitution system. J Exp Med. 2002;195:991-1001.
17. Dudziak D, Kamphorst AO, Heidkamp GF, et al. Differential antigen processing by dendritic cell subsets in vivo. Science. 2007;315:107-111.
18. Voehringer D, Rosen DB, Lanier LL, Locksley RM. CD200 receptor family members represent novel DAP12-associated activating receptors on basophils and mast cells. J Biol Chem. 2004;279: 54117-54123.
19. Martín-Fontecha A, Thomsen LL, Brett S, et al. Induced recruitment of NK cells to lymph nodes provides IFN-γ for T_H1 priming. Nat Immunol. 2004;12:1260-1265.
20. Poorafshar M, Helmby H, Troye-Blomberg M, Hellman L. MMCP-8, the first lineage-specific differentiation marker for mouse basophils: elevated numbers of potent IL-4-producing and MMCP-8-positive cells in spleens of malaria-infected mice. Eur J Immunol. 2000;30:2660-2668.
21. Fujita S, Seino K, Sato K, et al. Regulatory dendritic cells act as regulators of acute lethal systemic inflammatory response. Blood. 2006;107: 3656-3664.
22. Fujita S, Yamashita N, Ishii Y, et al. Regulatory dendritic cells protect against allergic airway inflammation in a murine asthmatic model. J Allergy Clin Immunol. 2008;121:95-104.
23. Boussiotis VA, Freeman GJ, Taylor PA, et al. $p27^{kip1}$ functions as an anergy factor inhibiting interleukin 2 transcription and clonal expansion of alloreactive human and mouse helper T lymphocytes. Nat Med. 2000;6:290-297.
24. Snelgrove RJ, Goulding J, Didierlaurent AM, et al. A critical function for CD200 in lung immune homeostasis and the severity of influenza infection. Nat Immunol. 2008;9:1074-1083.
25. Hatherley D, Cherwinski HM, Moshref M, Barclay AN. Recombinant CD200 protein does not bind activating proteins closely related to CD200 receptor. J Immunol. 2005;175:2469-2474.
26. Coombes JL, Siddiqui KR, Arancibia-Cárcamo CV, et al. A functionally specialized population of mucosal $CD103^+$DCs induces $Foxp3^+$ regulatory T cells via a TGF-β and retinoic acid-dependent mechanism. J Exp Med. 2007;204:1757-1764.
27. Yamazaki S, Bonito AJ, Spisek R, et al. Dendritic cells are specialized accessory cells along with TGF-β for the differentiation of $Foxp3^+$ $CD4^+$ regulatory T cells from peripheral $Foxp3^-$ precursors. Blood. 2007;110:4293-4302.
28. Sato K, Yamashita N, Baba M, Matsuyama T. Modified myeloid dendritic cells act as regulatory dendritic cells to induce anergic and regulatory T cells. Blood. 2003;101:3581-3589.